Lipid organization in xerosis: the key of the problem?

R. Vyumvuhore, R. Michael-Jubeli, L. Verzeaux, D. Boudier, M. Le Guillou, S. Bordes, D. Libong, A. Tfayli, M. Manfait, B. Closs

International Journal of Cosmetic Science

Lipid organization in xerosis: the key of the problem?

Journal:	*International Journal of Cosmetic Science*
Manuscript ID	Draft
Manuscript Type:	Original Article
Keywords:	Skin physiology/structure, skin barrier, Xerosis, spectroscopy, stratum corneum ceramides

R. Vyumvuhore, SILAB R&D Department, Brive, France

R. Michael-Jubeli, Université Paris-Sud, Paris, France

L. Verzeaux,SILAB R&D Department, Brive, France

D. Boudier, SILAB R&D Department, Brive, France

M. Le Guillou, SILAB R&D Department, Brive, France

S. Bordes, SILAB R&D Department, Brive, France

D. Libong, Université Paris-Sud, Paris, France

A. Tfayli, Université Paris-Sud, Paris, France

M. Manfait, BioSpecT, Biophotonique et Technologies pour la Santé, UMR CNRS 7369, Université de Reims Champagne Ardenne, Reims, France

B. Closs, SILAB R&D Department, Brive, France

ABSTRACT

OBJECTIVE

Although xerosis is a common skin disorder among the population, there is no *in vivo* global study focusing on healthy xerotic skin. Hence, the objective of this study was to characterize xerotic skin from the surface to the molecular scale with *in vivo* and non-invasive approaches.

METHODS

For this purpose, 15 healthy volunteers with normal skin and 19 volunteers with healthy xerotic skin were selected by a dermatologist thanks to a visual scorage. Firstly, the skin surface was characterized with biometric measurements. Then, the state of skin dryness was assessed by *in vivo* confocal microscopy. The molecular signature of xerotic skin was then determined by *in vivo* confocal Raman microspectroscopy. Finally, an identification of *stratum corneum* (SC) lipids was performed using Normal phase liquid chromatography (NP-LC) coupled to two detectors: Corona and /High Resolution Mass Spectroscopy (HR/MS).

RESULTS

Results obtained at the skin surface displayed an increase of the transepidermal water loss (TEWL) and a decrease of the hydration rate in xerotic skin. Confocal microscopy revealed an alteration of the cell shape in xerotic skin. Moreover, confocal Raman microspectroscopy demonstrated for the first time directly *in vivo* and non-invasively the lack of organization and conformation of lipids in this skin. Finally, HPLC analyses revealed that three ceramide sub-classes (NDS, NS and EOP) significantly decrease in xerosis. Altogether, these results identify parameters for the characterization of healthy xerotic skin compared to normal.

CONCLUSION

This study highlighted for the first time in dermo-cosmetic research, discriminative parameters from the surface to the molecular level *in vivo* and non-invasively between healthy xerotic and normal skins. These results will be useful for the development of new cosmetic active ingredients dedicated to xerotic skin.

KEY WORDS

Skin barrier

Skin physiology/structure

Spectroscopy

Molecular signature

Xerotic skin

Stratum Corneum Ceramides

INTRODUCTION

In healthy normal skin, the epidermis, and more precisely its upper layer the *stratum corneum* (SC), is involved in the protection against external aggressions such as pollutants, chemicals or micro-organisms (1,2). The SC is composed of end maturated keratinocytes annucleated, named corneocytes, that are surrounded by a lipid matrix ensuring the cellular cohesion (3) which is essential for the maintenance of the skin barrier permeability (4). Lipid synthesis occurs in the lamellar bodies of keratinocytes in all nucleated layers of the epidermis, and the newly synthesized and maturated lipids are delivered to the interstices of the SC during epidermal differentiation (5,6). Indeed, in a normal SC there is an equimolar proportion of ceramides (CER), cholesterol (CHOL) and free fatty acids (FFA) (7). The change in the lipid composition during the formation of the SC results in a very densely packed structure (8). Lipids play an irreplaceable role in skin barrier by avoiding water disruption and ensuring the hydration of the skin (9). The lipid organization is also essential for maintaining the skin barrier permeability. In healthy normal skin, lipids display an orthorhombic organization, corresponding to an important lipid compacity restraining the water disruption (8).

An alteration of the skin barrier is involved in some diseases such as atopic dermatitis, lamellar ichthyosis and Gaucher disease. These diseases are characterized by a pathological state of xerosis inducing an alteration of lipid organization and a breakdown of the skin barrier function (10,11). Recently, we identified *in vivo* and non-invasively a specific molecular signature of atopic skin compared to normal skin revealing a disruption of the lipid matrix in this pathology (12). Moreover, a study from Choi and Maibach demonstrate that CER are very important for a proper barrier function (13).

However, xerosis, so called dry skin, could also be observed in healthy skin. This is a common skin disorder that could be due to extrinsic (climate, environment, lifestyle) or intrinsic (hormones, disease) factors (14,15). Xerotic skin is visually characterized by a high dehydration inducing scales and rough surface (16). Moreover, a study conducted *ex vivo* by tape stripping revealed a significant decrease of ceramides level in xerotic skin, depending of the grade of the xerosis (17). These observations are related to a modification of the lipid composition and organization observed exclusively *ex vivo* up to date (18,19). Indeed, if there are experimentations performed *ex vivo* on xerotic skin, there is no global study comparing, from visual scorage to the molecular level, healthy xerotic and healthy normal skins.

The aim of our publication was thus to conduct a complete study directly *in vivo* and non-invasively on healthy volunteers to define parameters discriminating normal from xerotic skin. For this purpose, we firstly measured the biometric parameters and determined the dryness by confocal microscopy. Then, *in vivo* confocal Raman microspectroscopy characterized a spectral signature of xerotic skin. Finally, the lipid composition was determined using Normal phase liquid chromatography (NP-LC) coupled to two detectors: Corona and /High Resolution Mass Spectroscopy (HR/MS). Altogether, these results provide for the first time in dermo-cosmetic research a global study of healthy xerotic skin compared to normal.

EXPERIMENTAL DESIGN

Description of the panel

A first group of 15 healthy volunteers with normal skin (mean age: 58 years) and a second group of 19 healthy volunteers with xerotic skin (mean age: 57 years) were selected by a dermatologist. The dryness was visually evaluated under a standardized racking light by a trained expert according to a scale scoring from 1 (without dryness) to 4 (high level of dryness) as previously described (20). Volunteers involved in this study gave their written informed consent. Washing skin and application of topical products were prohibited 48 hours before measurements. *In vivo* measurements were performed on outside arms or the calf following 15 minutes of acclimation under control room conditions (22°C ± 2°C and 40% of relative humidity).

Biometric measurements

Transepidermal water loss (TEWL) was measured using Tewameter® TM210 (Courage & Khazaka electronic GmbH, Köln, Germany) and skin hydration was obtained with Corneometer® CM820 (Courage & Khazaka). To minimize the intra-individual variation, the presented TEWL and skin hydration values are the mean of 3 measurements for each subject.

In vivo confocal microscopy

Image acquisitions were obtained *in vivo* with a confocal microscope (Vivascope® 1500 Trilaser, Mavig GmbH, Munich, Germany) in fluorescence mode (445 nm) using fluorescein (Sigma, St. Louis, Mo, USA) as contrast agent. The SC was examined at each depth (z), starting from the surface of the epidermis (depth 0 µm) and descending down to a relative depth of 18 µm in 3 µm steps. Images were processing as previously

described by Guzman *et al* (21). A blind evaluation of reconstructed images was then performed by trained experts.

In vivo confocal Raman microspectroscopy

Raman investigations were performed using an *in vivo* confocal Raman microprobe (Horiba Jobin Yvon, Palaiseau, France) coupled to a dispersive Raman spectrometer (Micro HR, Horiba Jobin Yvon) and piloted with the software Labspec 5 software (Horiba Jobin Yvon). A description of this system is detailed in precedent studies (22). Raman profiles were collected from the surface to a relative depth of 30 µm. Five spectra were acquired by area of measurement and spectral data pre-processing was realized with Matlab® 7.2 (MathWorks, Natick, USA). Aberrant profiles were excluded by visual inspection of data. Selected profiles were submitted to a succession of corrections as previously described (12).

Identification of *Stratum Corneum* lipids

The *in vivo* SC lipid extraction was performed using the method previously described by C. Merle *et al.* (23). Lipid extracts were analyzed using a silica-grafted polyvinyl alcohol (PVA)-Sil column (PVA-bonded column; 5µm particle size, 150 x 4.6 mm) purchased from YMC (Kyoto, Japan). The HPLC system (Ultimate 3000 Dionex, Thermofisher Scientific, San Jose, CA) was coupled to Corona® CAD (ESA Biosciences, Chelmsford, USA). The analysis was performed using Chromeleon software. A NP-LC/HRMS analysis with an APCI in positive and negative mode was then conducted using an hybrid mass spectrometer LTQOrbitrap Velos Pro (Thermofisher Scientific, San Jose, CA) The molecular formula of lipids was obtained with the Xcalibur software (Thermo Scientific, Waltham, USA)

Statistical analyses

The distribution and the significance of results were respectively determined by Shapiro-Wilk and Wilcoxon tests with the Statgraphics software (Centurion).

Univariate analyses were obtained by Student's t test and considered as a non-significant difference if $P>0.05$. Values are considered significantly different and represented with * if $P<0.05$, ** if $P<0.01$ and *** if $P>0.001$.

Multivariate analysis "Partial Least Square-Discriminant Analysis" (PLS-DA) was conducted on data from volunteers taken into account biometrologicals and spectral variables. Data were normalized before analysis with the SIMCA-P 11 software (Umetrics, Umea, Sweden).

The randfeatures tests were used to characterize discriminating Raman frequencies between the groups of volunteers (normal skin and xerotic skin).

RESULTS

Comparison of healthy normal and xerotic skin surface parameters by using biometric measurements

We firstly compared the skin surface from normal and xerotic skins. Results displayed in the figure 1 highlight a significant increase of the TEWL (Fig.1a) and a decrease of the hydration level (Fig. 1b) in xerotic skin.

Comparison of healthy normal and xerotic skins at the cellular level by *in vivo* confocal microscopy

Then, cell morphologies in normal and xerotic skins were investigated by using *in vivo* confocal microscopy. Figure 2 corresponds to representative images of corneocytes in normal and xerotic skins. This figure reveals specific cell morphologies. Indeed, normal skin corneocytes have a hexagonal shape with a honeycomb structure while they have a rounded shape and a scale disposition in xerotic skin (Figure 2).

Comparison of healthy normal and xerotic skin molecular signature by *in vivo* confocal Raman microspectroscopy

To determine if xerotic skin had a specific molecular signature compared with normal skin, spectra obtained by *in vivo* confocal Raman microspectroscopy were obtained non-invasively on normal and xerotic skins. Figure 3 highlights significant differences between normal and xerotic skins at different wavenumbers (vertical lines) referring to the lipids. Indeed, bands between 1065 and 1130 cm^{-1} referring to the lipid organization display significant differences resulting in a lower density of cutaneous lipid structures in xerotic skin. Moreover, there is also significant differences around the spectral region of 1620-1680 cm^{-1}, corresponding to the stretching of amide I band. These differences

involved a modification in the chemical microenvironment of ceramides, thus inducing an impairment of the compactness of lamellar lipid structures with xerosis.

Comparison of healthy normal and xerotic skin lipid composition by HPLC

In order to go further in the characterization of xerotic skin, the composition of the lipid matrix was then analyzed by HPLC-Corona. The percentages of the three lipid classes of SC (fatty acids, cholesterol and ceramides) were relatively identical in both types of xerotic and normal skins. However, an evolution within ceramide micro-heterogeneity was observed. Results demonstrated a discrimination between some chromatographic peaks (data not shown). To strengthen and complete these results, a study by NP-LC/HRMS APCI was conducted. CER that were found to be involved in xerotic skin belong to three ceramide sub-classes: non-hydroxy fatty acid dihydrosphingosine (NdS), non-hydroxy fatty acid sphingosine (NS) and Esterified ω-hydroxy fatty acid phytosphingosine (EOP). In fact, 10 m / z ions varied significantly. But for the most part, the lack of sensitivity in negative mode did not allow a confirmation of the structures. Nevertheless, three EOP CER were identified with APCI negative and positive modes. Molecular ions in negative mode $[M+Cl]^-$ were m/z 1050.9163, 1064.9322 and 1078.9477. Moreover, molecular ions in positive mode $[M+H]^+$ were m/z 1016.95, 1030.97 and 1044.89. The corresponding determined raw formula were $C_{65}H_{126}NO_6$, $C_{66}H_{128}NO_6$ and $C_{67}H_{130}NO_6$ respectively. Results displayed in the Figure 4 illustrated the discriminatory character of these three types of CER which are substantially decreased in xerotic skin.

Multiparametric characterization of xerotic skin by using PLS-DA statistical analysis

A PLS-DA statistical analysis was performed with spectral variables and biometric measurements. Results displayed in the figure 5 revealed a significant discrimination according to the component 1 between normal and xerotic skins regarding spectral

variables and biometric measurements (SC lipid organization, compactness and composition, relative content in lipids, TEWL and hydration level).

DISCUSSION

If xerotic pathological skin is characterized at the molecular level, to our knowledge there was no study discriminating healthy normal from healthy xerotic skin *in vivo* and non-invasively. We thus conducted multiparameter analyses from biometric measurements to HPLC analyses through *in vivo* confocal microscopy and confocal Raman microspectroscopy. Firstly, the biometric parameters confirmed that volunteers selected by the dermatologist display skin surface characteristics of xerotic skin that are roughness and dryness (24). These results were confirmed by *in vivo* confocal microspectroscopy experiments revealing a modification of the cell shape in xerotic skin with a rounded shape and a scale disposition, in correlation with a disorganization of the skin barrier. Indeed, a similar change was also observed in a previous study we conducted on healthy skin with an altered skin barrier function by Sodium Lauryl Sulfate, known to disrupt the skin barrier (21).

Previous studies, conducted *ex vivo* and invasively, report an alteration of the lipid matrix in xerotic skin (18,19). Indeed, the SC lipid matrix ensures the skin barrier function avoiding the water disruption (4). However, to our knowledge, no data was available on the *in vivo* characterization of the lipid matrix in healthy xerotic skin compared to healthy normal skin. *In vivo* confocal Raman microspectroscopy is an adapted tool to analyze specific molecular descriptors of the SC (25). Indeed, this approach allowed us to recently characterize for the first time *in vivo* and non-invasively the molecular signature of atopic skin (12). The analysis of the spectra highlighted that lipids of the SC were significantly modified in healthy xerotic skin. Indeed, the lipid content was decreased and the lipid organization and compactness were impaired with xerosis. These results confirmed the alteration of the normal orthorhombic organization of the lipid matrix *in vivo* and could explain the water loss measured in healthy xerotic skin. To go further in the study of this skin disorder, the lipid composition was then

analyzed. For this purpose, we used liquid chromatography, a technique previously used to characterize lipid composition in normal skin (23). Results determined that three CER were mainly deficient in xerotic skin. Comparatively to normal skin, the decrease of these CER revealed a change in the structural micro-heterogeneity of SC lipids with xerosis. This modification is in correlation with an alteration of the skin barrier function (26).

Hence, this *in vivo* and non-invasive multiparameter analysis allowed for the first time in dermo-cosmetic research to characterize xerotic skin from visual to molecular level. Altogether, these results allowed a better understanding of xerotic skin, a healthy skin condition not yet characterized *in vivo* and non-invasively. This study will enable the development of specific cosmetic active ingredients dedicated to healthy xerotic skin.

FIGURES

Figure 1. Modification of skin surface parameters in xerotic skin. a. Measurement of the TEWL with a Tewameter® at the surface of normal and xerotic skins. b. Measurement of the hydration level with a Corneometer® at the surface of normal and xerotic skins. Statistical analyses were determined by Student's t test with ***: P<0.001.

Figure 2. Modification of the cell morphology in xerotic skin. Confocal microscopy images and analysis of the corneocytes morphologies in normal and xerotic skins.

Figure 3: Modification of the molecular signature in xerotic skin. Analysis of confocal Raman microspectroscopy spectra of normal and xerotic skins with a Randfeatures statistical analyses (P<0.05).

Figure 4: Study of the HPLC signal intensity for the three EOP CER in normal and xerotic skins. Statistical analyses were determined by Student's t test with *: P<0.05.

Figure 5: Analysis of spectral variables and biometric measurements with a Partial Least Square-Discriminant Analysis (PLS-DA).

BIBLIOGRAPHY

1. Madison KC. Barrier function of the skin: « la raison d'être » of the epidermis. J Invest Dermatol. 2003;121(2):231‐41.

2. Baroni A, Buommino E, De Gregorio V, Ruocco E, Ruocco V, Wolf R. Structure and function of the epidermis related to barrier properties. Clin Dermatol. 2012;30(3):257‐62.

3. Nemes Z, Steinert PM. Bricks and mortar of the epidermal barrier. Exp Mol Med. 1999;31(1):5‐19.

4. Feingold KR, Elias PM. Role of lipids in the formation and maintenance of the cutaneous permeability barrier. Biochim Biophys Acta. 2014;1841(3):280‐94.

5. Castiel-Higounenc I, Chopart M, Ferraris C. Stratum corneum lipids: specificity, role, deficiencies and modulation. OCL. 2004;11(6):401‐6.

6. Proksch E, Holleran WM, Menon GK, Elias PM, Feingold KR. Barrier function regulates epidermal lipid and DNA synthesis. Br J Dermatol. 1993;128(5):473‐82.

7. Weerheim A, Ponec M. Determination of stratum corneum lipid profile by tape stripping in combination with high-performance thin-layer chromatography. Arch Dermatol Res. 2001;293(4):191‐9.

8. Bouwstra JA, Ponec M. The skin barrier in healthy and diseased state. Biochim Biophys Acta. 2006;1758(12):2080‐95.

9. Mutanu Jungersted J, Hellgren LI, Høgh JK, Drachmann T, Jemec GBE, Agner T. Ceramides and barrier function in healthy skin. Acta Derm Venereol. 2010;90(4):350‐3.

10. Holleran WM, Ginns EI, Menon GK, Grundmann JU, Fartasch M, McKinney CE, et al. Consequences of beta-glucocerebrosidase deficiency in epidermis. Ultrastructure and permeability barrier alterations in Gaucher disease. J Clin Invest. 1994;93(4):1756‐64.

11. Hara J, Higuchi K, Okamoto R, Kawashima M, Imokawa G. High-expression of sphingomyelin deacylase is an important determinant of ceramide deficiency leading to barrier disruption in atopic dermatitis. J Invest Dermatol. 2000;115(3):406‐13.

12. Verzeaux L, Vyumvuhore R, Boudier D, Le Guillou M, Bordes S, Essendoubi M, et al. Atopic skin: In vivo Raman identification of global molecular signature, a comparative study with healthy skin. Exp Dermatol. 2017;

13. Choi MJ, Maibach HI. Role of ceramides in barrier function of healthy and diseased skin. Am J Clin Dermatol. 2005;6(4):215‐23.

14. Pons-Guiraud A. Dry skin in dermatology: a complex physiopathology. J Eur Acad Dermatol Venereol JEADV. 2007;21 Suppl 2:1‐4.

15. Barco D, Giménez-Arnau A. Xerosis: a dysfunction of the epidermal barrier. Actas Dermo-Sifiliográficas. 2008;99(9):671‐82.

16. Engelke M, Jensen JM, Ekanayake-Mudiyanselage S, Proksch E. Effects of xerosis and ageing on epidermal proliferation and differentiation. Br J Dermatol. 1997;137(2):219–25.

17. Lu N, Chandar P, Tempesta D, Vincent C, Bajor J, McGuiness H. Characteristic differences in barrier and hygroscopic properties between normal and cosmetic dry skin. I. Enhanced barrier analysis with sequential tape-stripping. Int J Cosmet Sci. 2014;36(2):167–74.

18. Schreiner V, Gooris GS, Pfeiffer S, Lanzendörfer G, Wenck H, Diembeck W, et al. Barrier characteristics of different human skin types investigated with X-ray diffraction, lipid analysis, and electron microscopy imaging. J Invest Dermatol. 2000;114(4):654–60.

19. Pennick G, Chavan B, Summers B, Rawlings AV. The effect of an amphiphilic self-assembled lipid lamellar phase on the relief of dry skin. Int J Cosmet Sci. 2012;34(6):567–74.

20. Byrne AJ. Bioengineering and subjective approaches to the clinical evaluation of dry skin. Int J Cosmet Sci. 2010;32(6):410–21.

21. Guzman A, Boudier D, Breugnot J, Rondeau D, Le Guillou M, Closs B. An Innovative, Rapid, Qualitative and Quantitative Approach to the Epidermal Barrier Function with In Vivo Confocal Laser Scanning Microscopy. IFSCC Mag. 2013;16(3):157–63.

22. Vyumvuhore R, Tfayli A, Piot O, Le Guillou M, Guichard N, Manfait M, et al. Raman spectroscopy: in vivo quick response code of skin physiological status. J Biomed Opt. 2014;19(11):111603.

23. Merle C, Laugel C, Chaminade P, Baillet-Guffroy A. Quantitative Study of the Stratum Corneum Lipid Classes by Normal Phase Liquid Chromatography: Comparison Between Two Universal Detectors. J Liq Chromatogr Relat Technol. 2010;33(5):629–44.

24. Berry N, Charmeil C, Goujon C, Silvy A, Girard P, Corcuff P, et al. A Clinical, Biometrological and Ultrastructural Study of Xerotic Skin. Int J Cosmet Sci. 1999;21(4):241–52.

25. Eklouh-Molinier C, Gaydou V, Froigneux E, Barlier P, Couturaud V, Manfait M, et al. In vivo confocal Raman microspectroscopy of the human skin: highlighting of spectral markers associated to aging via a research of correlation between Raman and biometric mechanical measurements. Anal Bioanal Chem. 2015;407(27):8363–72.

26. van Smeden J, Janssens M, Gooris GS, Bouwstra JA. The important role of stratum corneum lipids for the cutaneous barrier function. Biochim Biophys Acta. 2014;1841(3):295–313.

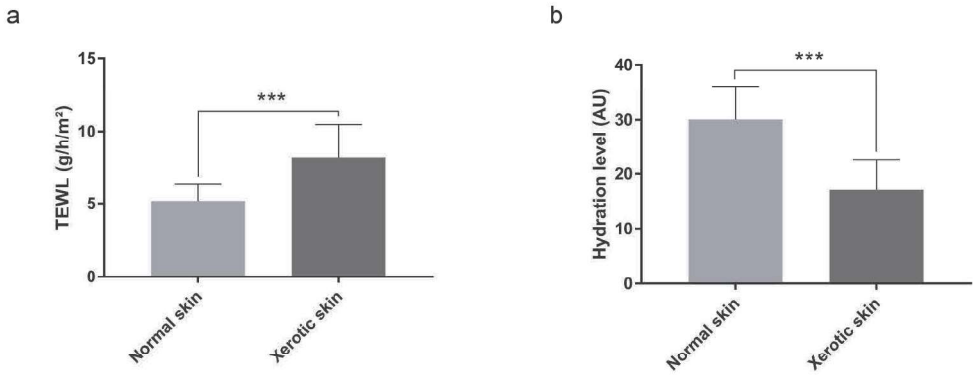

Figure 1. Modification of skin surface parameters in xerotic skin. a. Measurement of the TEWL with a Tewameter® at the surface of normal and xerotic skins. b. Measurement of the hydration level with a Corneometer® at the surface of normal and xerotic skins. Statistical analyses were determined by Student's t test with ***: P<0.001.

221x85mm (300 x 300 DPI)

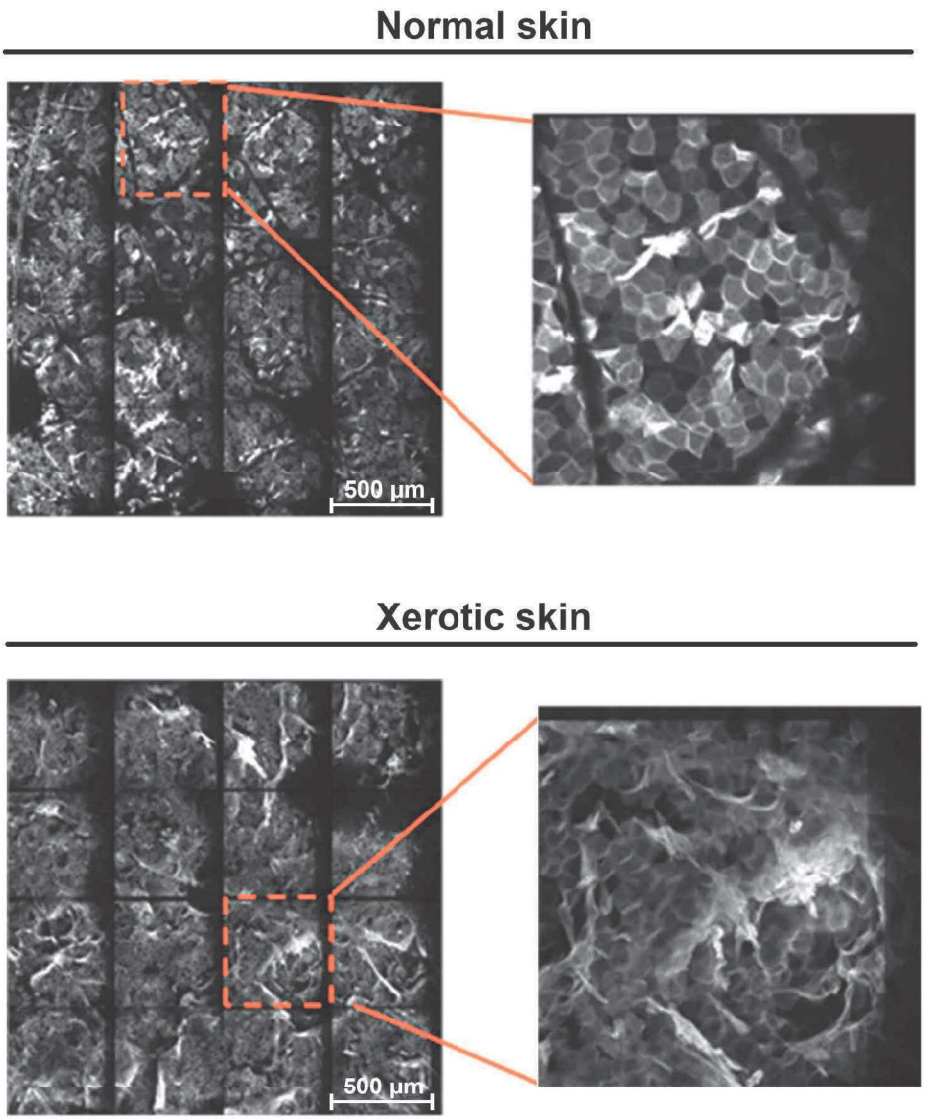

Figure 2. Modification of the cell morphology in xerotic skin. Confocal microscopy images and analysis of the corneocytes morphologies in normal and xerotic skins.

191x225mm (300 x 300 DPI)

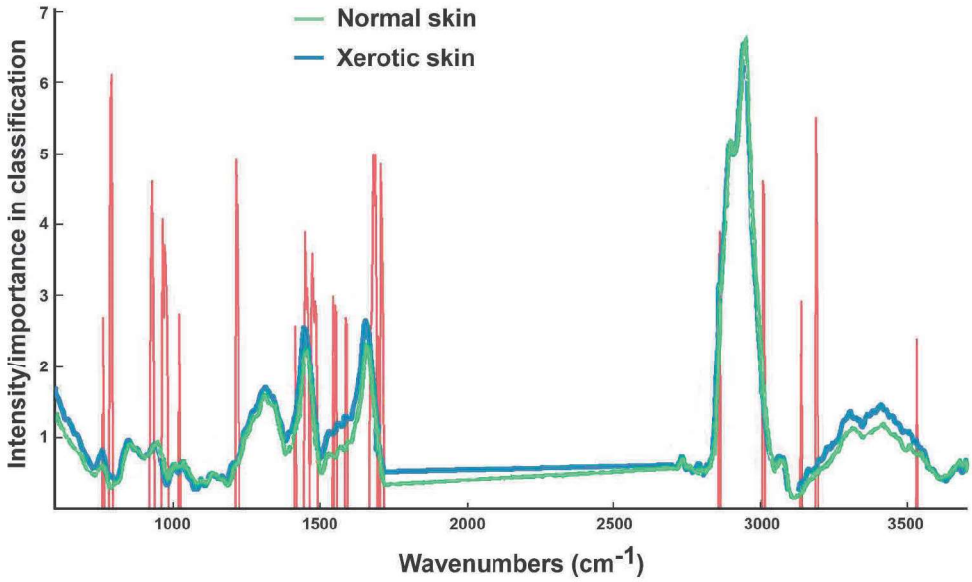

Figure 3: Modification of the molecular signature in xerotic skin. Analysis of confocal Raman microspectroscopy spectra of normal and xerotic skins with a Randfeatures statistical analyses (P<0.05).

224x138mm (300 x 300 DPI)

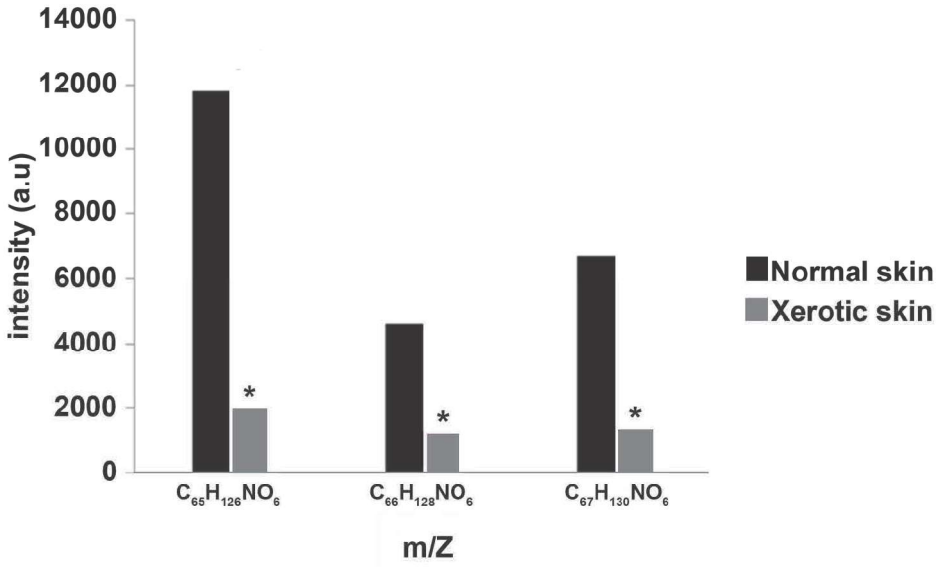

Figure 4: Study of the HPLC signal intensity for the three EOP CER in normal and xerotic skins. Statistical analyses were determined by Student's t test with *: P<0.05.

160x94mm (300 x 300 DPI)

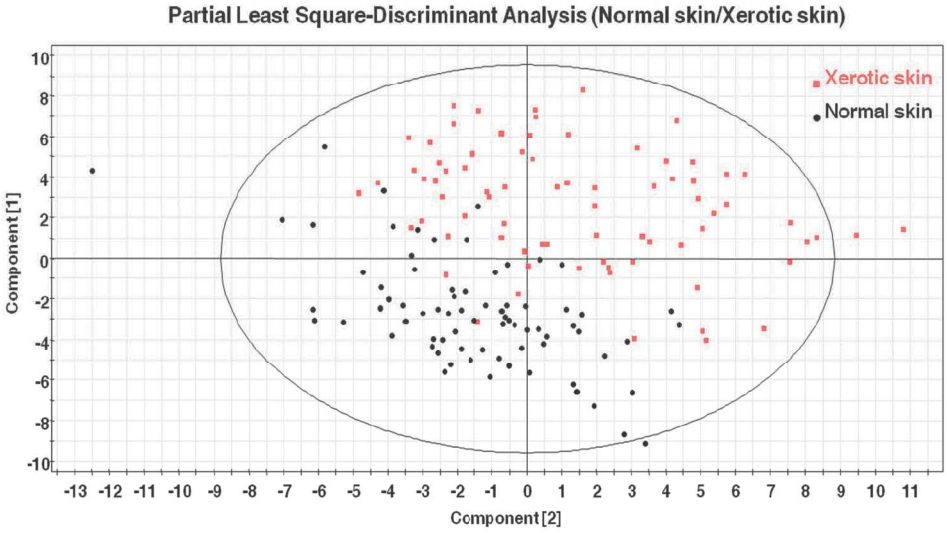

Figure 5: Analysis of spectral variables and biometric measurements with a Partial Least Square-Discriminant Analysis (PLS-DA).

147x84mm (300 x 300 DPI)